

An investigation of the performance of the waveguide superconducting HEB mixer at different RF embedding impedances

D. Loudkov, C.-Y.E. Tong, R. Blundell, N. Kaurova, E. Grishina, B. Voronov, G. Gol'tsman

Abstract — We have conducted an investigation of the performance of superconducting hot-electron bolometric (HEB) mixer at 800 GHz as a function of the embedding impedance of the waveguide embedding circuit. Using a single half-height mixer block, we have developed three different mixer chip configurations, offering nominal embedding resistances of 70, 35, and 15 Ohms. Both the High Frequency Structure Simulator (HFSS) software and scaled model impedance measurements were employed in the design process. Two batches of HEB mixers were fabricated to these designs using 3-4 nm thick NbN thin film. The mixers were characterized through receiver noise temperature measurements and Fourier Transform Spectrometer (FTS) scans. Briefly, a minimum receiver noise temperature of 440 K was measured at a local oscillator frequency 850 GHz for a mixer of normal state resistance 62 Ohms incorporated into a circuit offering a nominal embedding impedance of 70 Ohms. We conclude from our data that, for low noise operation, the normal state resistance of the HEB mixer element should be close to that of the embedding impedance of the mixer mount.

Index Terms— Hot-electron bolometer mixer, Embedding impedance, Fixed-tuned waveguide receiver,

I. INTRODUCTION

HOT Electron Bolometer (HEB) based receivers currently offer the highest sensitivity above 1.2 THz. These receivers have been selected for a number of astronomical instruments in the Terahertz frequency range [1-5]. The lowest receiver noise temperatures reported for laboratory prototypes are of the order of $(10h\nu/k)$ [6, 7].

In the design of HEB mixers, it has been generally assumed that the impedance of the HEB element is real. This

D. Loudkov is with the Moscow State Pedagogical University, Moscow, Russia, 119992 (e-mail: dloudkov@cfa.harvard.edu).

C.-Y. E. Tong is with the Harvard-Smithsonian Center for Astrophysics, Cambridge, MA 02138 (e-mail: etong@cfa.harvard.edu).

R. Blundell is with the Harvard-Smithsonian Center for Astrophysics, Cambridge, MA 02138 (e-mail: rblundell@cfa.harvard.edu).

N. Kaurova is with the Moscow State Pedagogical University, Moscow, Russia, 119992 (e-mail: nkaurova@mail.ru).

E. Grishina is with the Moscow State Pedagogical University, Moscow, Russia, 119992 (e-mail: Grishina@front.ru).

B. Voronov is with the Moscow State Pedagogical University, Moscow, Russia, 119992 (e-mail: bmvoronov@mail.ru).

G. Gol'tsman is with the Moscow State Pedagogical University, Moscow, Russia, 119992 (e-mail: goltsman00@mail.ru).

impedance is considered to be close to the DC bias resistance at frequencies between the 3 dB gain roll-off and the energy gap of the superconducting film [8, 9]. At higher frequencies the film appears as a normal conductor and therefore, it may be logical to assume that the impedance at Terahertz frequencies is just the normal state resistance of the HEB element [10]. According to the BCS theory the relation between the energy gap at absolute zero and the critical temperature of a superconductor is: $2\Delta_0=3.52k_B T_c$. With $T_c=10$ K, the frequency corresponding to the superconducting energy gap is 0.74 THz. Since the HEB mixer operates in the resistive state, heated by DC bias current and incident Local Oscillator (LO) power, the effects of superconductivity are suppressed. It follows that the gap frequency is shifted down to lower frequencies. However, there exist only limited experimental data to support these assumptions.

We present an investigation of the optimal RF impedance of the waveguide HEB mixers designed for a center frequency of 0.8 THz. The devices were fabricated from 3.5 nm thick Niobium Nitride (NbN) film. We compare the performances of three different mixer chip designs, which present different source impedance to the HEB mixers.

II. CHIP DESIGN FOR THE WAVEGUIDE HEB MIXER

A scaled model was used to evaluate designs for our 0.8 THz waveguide mixer. The scaled model dimensions were 160 times larger than those of the actual mixer block such that model measurements were made at around 5 GHz. The mixer block design was adopted from mixer assembly of fixed tuned SIS mixer developed for the SubMillimeter Array telescopes [11, 12].

Three mixer chip configurations were designed by the High Frequency Structure Simulator (HFSS) software and confirmed by the scaled model measurements. The nominal impedances of these 3 designs are: 70 Ω (Design A), 35 Ω (Design B), and 15 Ω (Design C). The impedance value of design A is chosen to be close to the HEB mixer normal state resistance (R_N). For design C the embedding impedance is closest to the DC resistance at the optimal bias point (R_{DC}). With these three designs, the embedding impedances cover most of the range of interest for the HEB mixer.

At the target frequency of 800 GHz (5 GHz on the scaled model), the calculated complex impedances for the 3 designs are: 69 - j8 Ω , 37 + j2 Ω , 14 - j7 Ω respectively. All three

designs employ the same mixer chip dimensions and the mechanical design of the mixer block is also the same. The only difference lies in the detailed geometry of the electrodes of the HEB element which forms the coupling structure to the wave propagating down the waveguide. Consequently, the mixer chips are interchangeable and all three types of chip can be fabricated and processed, lapped and diced, at the same time on a single wafer.

The embedding impedance at the mixer feed point is derived from the scaled model vector measurement using the 3-standard de-embedding method [13]. For each design we first measure the reflection coefficient at the input port of the scaled model mixer mount with the mixer feed point terminated using the 3 known standards: an open, a short, and a 50Ω chip resistor. The embedding impedance is related to these reflection coefficients through the relation:

$$Z_{emb} = Z_r(\Gamma_o - \Gamma_r)/(\Gamma_r - \Gamma_s),$$

where Z_{emb} is the embedding impedance seen at the HEB mixer feed point, $Z_r = 50 \Omega$, and Γ is the measured reflection coefficient at the mixer input port for the three terminations: open (o), short (s) and 50Ω resistive (r) load. We obtained reasonable agreement between the impedances obtained by scaled model measurements and the impedances obtained by HFSS simulations.

III. HEB MIXERS

A photo mask incorporating all three designs was prepared, and e-beam lithography was used to fabricate two batches of mixer elements with dimensions $3 \times 0.15 \mu\text{m}^2$ and $3 \times 0.18 \mu\text{m}^2$ on 3-4 nm thick NbN film [14]. The critical temperature of superconducting transition, T_C , was about 10 K for the measured samples. All of the tested mixers have normal state resistances (R_N) of around 60Ω , extracted from the over-pumped current-voltage characteristics at 4.2 K.

Devices from batches I and II demonstrate considerable differences in their optimal bias conditions. For example, the DC resistance at the optimal bias point, defined as ($R_{DC} = V_{bias}/I_{bias}$), is generally around 24Ω for mixers from batch I but it is about 15Ω for batch II devices. Also, the differential resistance at the optimal bias point for batch I mixers ranges from 100 to 125Ω , but for batch II devices this generally lies between 60 and 90Ω . We believe that this behavior reflects variations in film quality between batches and a variation in contact resistance across the superconductor - normal metal interface.

Table I summarizes the characteristics of the HEB devices used in our experiments. The receiver input bandwidth (BW) was estimated from Fourier Transform Spectrometer (FTS) scans, which was made by using the mixer as a direct detector. For the receiver noise measurements (T_{RX}) we used an IF of 1.5 GHz, and included an isolator between the mixer and low-noise amplifier to present an in-band impedance of about 50Ω to the mixer. Y-factor measurements were performed in the frequency range from 770 GHz to 860 GHz with frequency step about 10 GHz using the same experimental set-up. The

minimum noise temperature measured for each device (Min T_{RX}) is given in the last column of Table I. These values are close to $10h\nu/k$, for mixer designs A and B, and are consistent with the highest reported sensitivities for this type of mixer [6, 7].

TABLE I
HEB MIXER CHARACTERISTICS

Device ^a	Z_{emb} (Ω)	R_{DC} @ opt bias (Ω)	R_N (Ω)	Input BW (GHz)	Min. T_{RX} (K)
AI#8	70	15	62	350	440
AI#17	70	14	72	350	480
AII#2	70	26	58	350	530
BI#13	35	13	50	330	470
BII#1	35	26	60	330	560
CII#13	15	21	51	220	603
CI#14	15	13	62	200	780

^aThe first letter of the device type indicates the chip design (A, B, or C), the roman numeral I or II indicates the batch number.

In figures 3, 4 and 5 we display the frequency response obtained from FTS scans for a variety of devices and the results of the Y-factor measurements (for 295K and 77K input loads to the receiver) are overlaid on the frequency response. From the FTS spectra, we note a low frequency cut-off, at around 600 GHz, which is due to the waveguide dimensions. Since the exact width and thickness of the individual mixer chip dictates the onset of higher order modes, the high frequency response of the mixers (above ~ 900 GHz) does not show a definite pattern.

In Fig. 3, we compare the response of two mixer chips of design A. We note a significant difference in performance between mixers AI#8 and AII#2, even though they possess almost identical R_N and critical current of 0.238 mA.

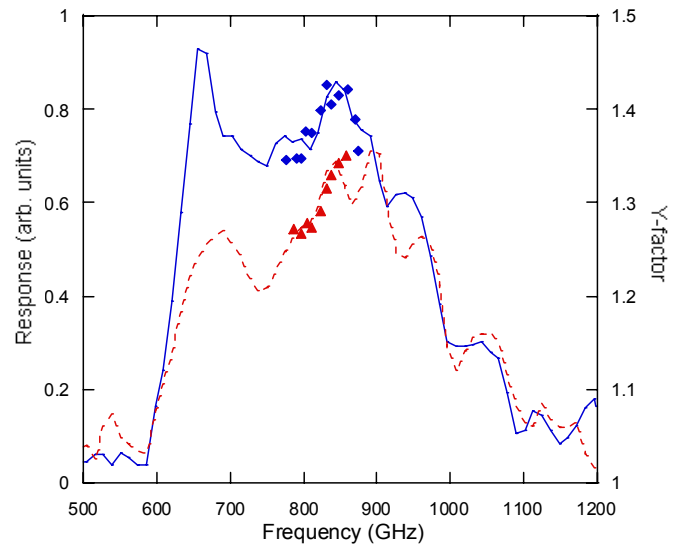


Fig. 3. Direct detector response and Y-factor values (symbols and right axis) of design A HEB mixers. The solid line and diamond symbols are for mixer AI#8, dashed line and triangles for mixer AII#2.

This suggests that some other additional, batch-dependent parameters play an important role in determining overall mixer performance. In other words, it is only possible to make a fair comparison of the performance of the different mixer designs from within a given batch.

In Fig. 4 we compare the FTS response of the three mixer types from the batch I. Referring to Table I, these mixers all have similar values of R_N . Mixer AI#8 has the best sensitivity among all of the measured devices. For example, at a local oscillator frequency of 850 GHz we measured a Y-factor of 1.42. This corresponds to a DSB receiver noise temperature of 440 K, or about $11 h\nu/k$. The input bandwidth for this mixer of ~ 350 GHz is also quite wide.

Mixer BI#13 has similar sensitivity and RF bandwidth to AI#8. This can be explained by the fact that the normal state resistance of each mixer is close to the embedding impedance. For device AI#8, the match between R_N and the nominal embedding impedance of 70Ω is better than 20 dB, and for BI#13, with a normal resistance of 50Ω and a nominal embedding impedance of 35Ω , we have a match of about 15 dB. Mixer CI#14 is significantly less sensitive and it has a narrower bandwidth than type A or B devices. For this mixer, the match between R_N and the nominal embedding impedance of 15Ω is only about 5 dB. Interestingly, the 13Ω DC resistance of this mixer at the optimal bias point is quite close to the nominal embedding impedance of 15Ω for the type C mixer.

Clearly for devices with $R_N \sim 60 \Omega$, designs A and B are better. This suggests that the optimal embedding impedance for low-noise performance should be close to the normal state resistance of the HEB element, not its DC resistance. However, the available data also suggest that the performance is not a very sharp function of the impedance match. Most likely, a match of better than 10-12 dB is quite sufficient.

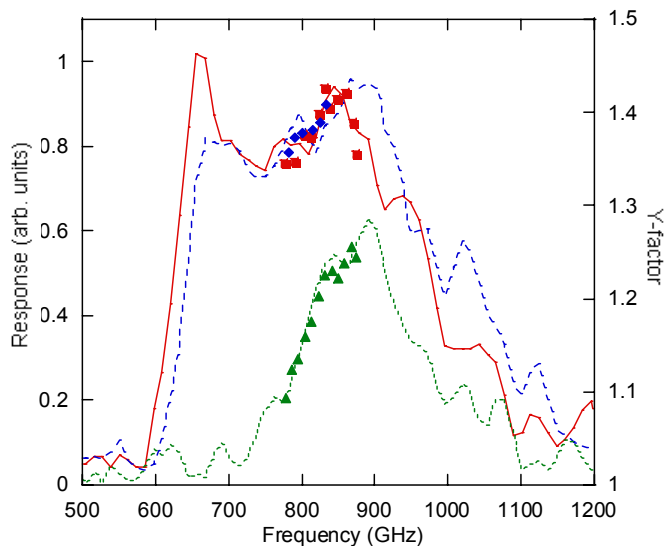


Fig. 4. Direct detector response and Y-factor (symbols and right axle) of the three types HEB mixer from batch I. The solid line and squares are for mixer AI#8, dashed line and diamonds for mixer BI#13, and dotted line and triangles for mixer CI#14.

In Fig. 5 we compare the performances of another set of devices, this time from batch II. Referring once more to Table I, the normal state resistance of these devices (AII#2, BII#1 and CII#13) has an almost identical spread to those from batch I. Mixers AII#2 and BII#1 have similar normal resistance (58Ω and 60Ω) and identical critical current (0.237 mA) which

indicate similar critical temperatures of the superconducting transition. Nevertheless, these two mixers possess different RF characteristics. The poorer performance of the type B mixer at low frequencies is undoubtedly a result of the difference in embedding impedance of the 2 mixer chips. At around 800 GHz, mixer CII#13 offers sensitivity close to that of the other two mixer types. However, it is less sensitive at low frequencies, and its RF bandwidth is much reduced. We can conclude that operating a mixer with R_N significantly different to the embedding impedance generally results in a reduction in sensitivity and RF bandwidth.

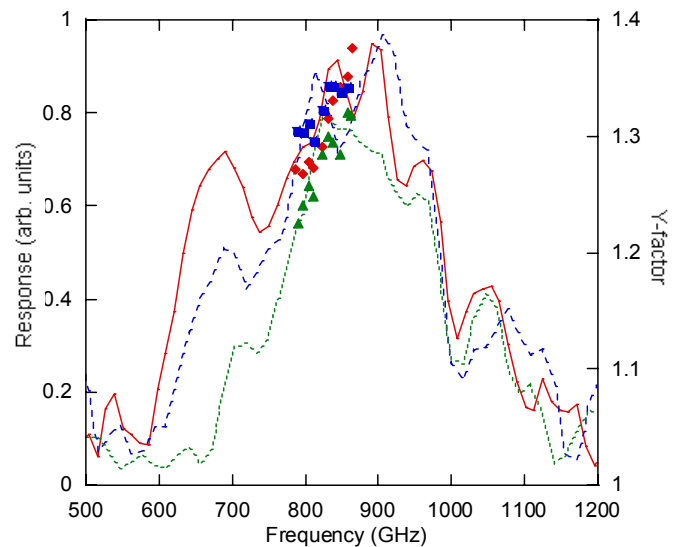


Fig. 5. Direct detector response and Y-factor (symbols and right axle) of the three types of HEB mixer from batch II. The solid line and diamonds are for mixer AII#2, dashed line and squares for mixer BII#1, and dotted line and triangles for mixer CII#13.

IV. SUMMARY

We have designed and fabricated three different types of waveguide HEB mixer chips, with nominal embedding impedance levels of 70Ω , 35Ω and 15Ω . For the mixer AI#8 with normal resistance value of 62Ω , designed for an embedding impedance of 70Ω , we have measured a DSB receiver noise temperature of 440 K at a local oscillator frequency 850 GHz. This corresponds to a sensitivity close to $10 h\nu/k$. Type A mixers offer an input bandwidth of about 350 GHz.

By comparing the sensitivity and frequency response of the different mixer types, we find that HEB mixers operate best with a normal state resistance close to that of the embedding network. However, RF performance is not a critical function of the match, but for $R_N \gg Z_{emb}$ the receiver sensitivity drops and the available input bandwidth is also reduced.

Our experimental data also confirms that other factors, such as film quality and contact resistance at the superconductor – normal metal interface can have a significant impact on the performance of the HEB mixer receiver.

REFERENCES

- [1] D. Meledin, D. Marrone, E. Tong, H. Gibson, R. Blundell, S. Paine, C. Papa, M. Smith, T. Hunter, J. Battat, B. Voronov, and G. Goltsman, "A 1-THz superconducting Hot-Electron-Bolometer Receiver for Astronomical Observations." *In press IEEE Trans. On Microwave Theory and Tech.*, vol. 52, no. 10, October 2004.
- [2] D. Marrone, R. Blundell, H. Gibson, S. Paine, D. C. Papa, C.-Y. E. Tong, "Characterization and Status of a Terahertz Telescope." *Proc. of the 15th International Symposium on Space Terahertz Technology*, Northampton, Massachusetts, USA, April 27-29, 2004.
- [3] K. Yngvesson, C. Musante, M. Rodriguez, Y. Zhuang, E. Gerecht, M. Coulombe, J. Dickinson, T. Goyette, J. Waldmann, C. Walker, A. Stark, A. Lane, "Terahertz receiver with NbN HEB device (TREND) – a low noise receiver user instrument for AST/RO at the south pole." *Proc. of the 12th Intern. Symposium on Space THz Technology*, p.26, San Diego, CA, 2001.
- [4] S. Cherednichenko, M. Kroug, H. Merkel, P. Khosropanah, A. Adam, E. Kollberg, D. Loudkov, G. Gol'tsman, B. Voronov, H. Richter, H.-W. Huebers, "1.6 THz heterodyne receiver for the far infrared space telescope", *Physica C*, Volume 372, p. 427-431, August 2002.
- [5] A. Semenov, H. Richter, K. Smirnov, B. Voronov, G. Gol'tsman, H.-W. Hübers, "The development of terahertz superconducting hot-electron bolometric mixers", *Superconductor Science and Technology*, Volume 17, Issue 5, pp. S436-S439, 2004.
- [6] C.-Y. E. Tong, J. Stern, K. Megerian, H. LeDuc, T.K. Sridharan, H. Gibson, R. Blundell, "A Low-noise NbTiN Hot Electron Bolometer Mixer." *Proc. of the 12th International Symposium on Space Terahertz Technology*, pp. 253-261, San Diego, CA, 2001.
- [7] M. Kroug, S. Cherednichenko, M. Choumas, H. Merkel, E. Kollberg, B. Voronov, G. Goltsman, D. Loudkov, H. W. Hubers, H. Richter, "HEB quasi-optical heterodyne receiver for terahertz frequencies," *Proc. of the 12th International Symposium on Space Terahertz Technology*, pp. 244-253, San Diego, CA, 2001.
- [8] H. Ekström, B. Karasik, E. Kollberg, S. Yngvesson, "Conversion gain and noise of niobium superconducting hot-electron bolometer mixers," *IEEE Trans. Microwave Theory and Tech.*, pp. 938-947, vol. 43, no. 4, april 1995.
- [9] B. S. Karasik, A. I. Elantev, "Analysis of the noise performance of a hot-electron bolometer mixer," *6th International Symposium on Space Terahertz Technology*, pp. 229-247, Pasadena, CA, 1995.
- [10] H. Ekstrom, E. Kollberg, P. Yagoubov, G. Goltsman, E. Gershenzon, and S. Yngvesson, "Gain and Noise Bandwidth of NbN Hot Electron Bolometric Mixers," *Appl. Phys. Lett.*, 70(24), 16 June 1997.
- [11] E. Tong, R. Blundell, S. Paine, D.C. Papa, J. Kawamura, R. Leombruno, X. Zhang, and J. Stern, H. LeDuc, "Design and characterization of a 250-350-GHz fixed-tuned superconductor-insulator-superconductor receiver," *IEEE Trans. Microwave Theory Tech.*, vol. 44, pp. 1548-1556, 1996.
- [12] J. Kawamura, R. Blundell, E. Tong, D.C. Papa, T. Hunter, S. Paine, F. Patt, G. Goltsman, S. Cherednichenko, B. Voronov, and E. Gershenzon, "Superconductive hot-electron bolometer mixer receiver for 800 GHz operation," *IEEE Trans. Microwave Theory Tech.*, vol. 48, pp. 683-689, 2000.
- [13] W. Zhang, C.-Y.E. Tong, S.C. Shi, "Scaled model measurement of the embedding impedance of a 660-GHz waveguide SIS mixer with a 3-standard deembedding method," *IEEE Microwave & Wireless Components Lett.*, vol. 13(9), pp. 376-378, Sept. 2003.
- [14] D. Meledin, C.-Y. E. Tong, R. Blundell, N. Kaurova, K. Smirnov, B. Voronov, G. Gol'tsman, "Study of the IF bandwidth of NbN HEB mixers based on crystalline quartz substrate with an MgO buffer layer", *IEEE Trans. Applied Superconductivity*, Vol. 13, p. 164, June 2003.